Supporting Information

Formation of Linear Plasmonic Heterotrimers Using Nanoparticle Docking to DNA Origami Cage

Yehan Zhang,[1] A'Lester C. Allen,[2] Zachary J. Petrek,[1] Huan H. Cao,[1] Devanshu Kumar,[1] Melissa C. Goodlad,[1] Vianna G. Martinez,[1] Jasdip Singh,[1] Jin Z. Zhang,[2,] and Tao Ye,[1,*]*

[1] Department of Chemistry and Biochemistry, University of California, Merced, California, 95343, United States

[2]Department of Chemistry and Biochemistry, University of California, Santa Cruz, California 95064, United States

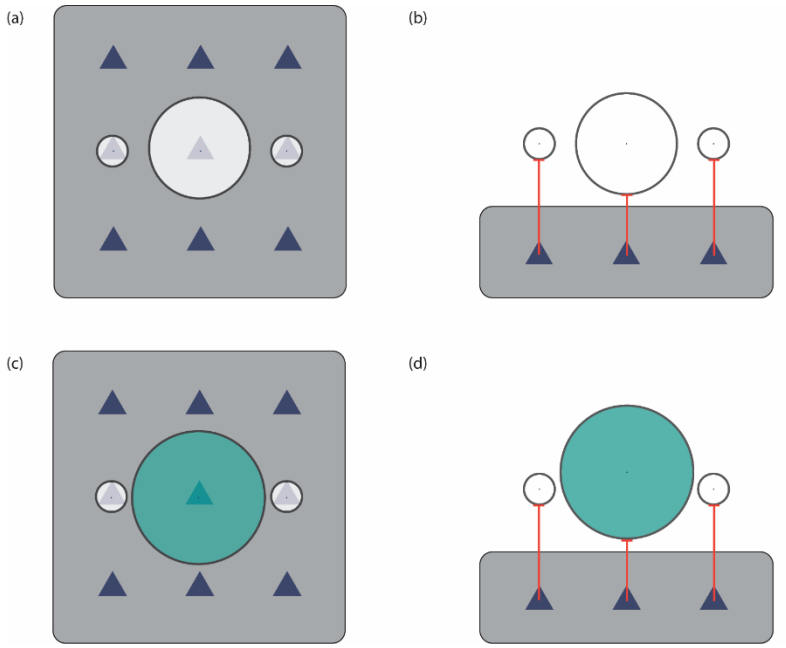

Figure S1. Schematic of polydisperse nanoparticles assembled on a DNA origami template. (a) Top view: Three nanoparticles with nominal sizes (white spheres) bound to the template surface (grey square: 2D tiles, blue triangle: binding site). (b) Side view: Three nanoparticles with nominal sizes bound to the template surface (red line: capture strand). The centers of three nanoparticles may be colinear when the capture strands for the smaller nanoparticles can be lengthened. (c) Top view showing that when the central nanoparticle (green sphere) is larger than its nominal size, interparticle gaps become smaller. (d) Side view showing that the bond angle also depends on the nanoparticle sizes. The centers of three nanoparticles are no longer colinear when one or more nanoparticles deviate from their nominal sizes.

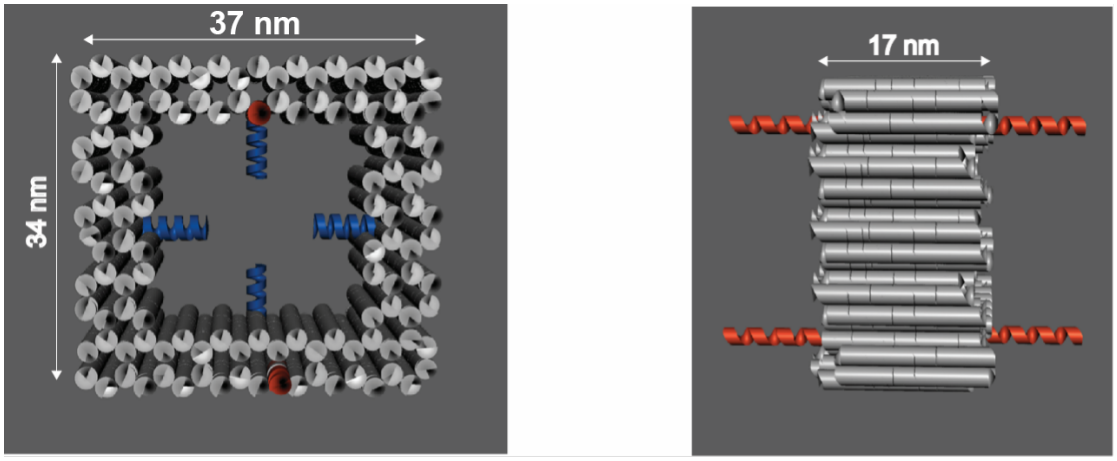

Figure S2. Dimensions of 3D hollow origami cage (assuming hydrated 2.2 nm helix width and 3.4 nm of helical turn length). Blue helices are inner capture strands, red helices are outside capture strands.

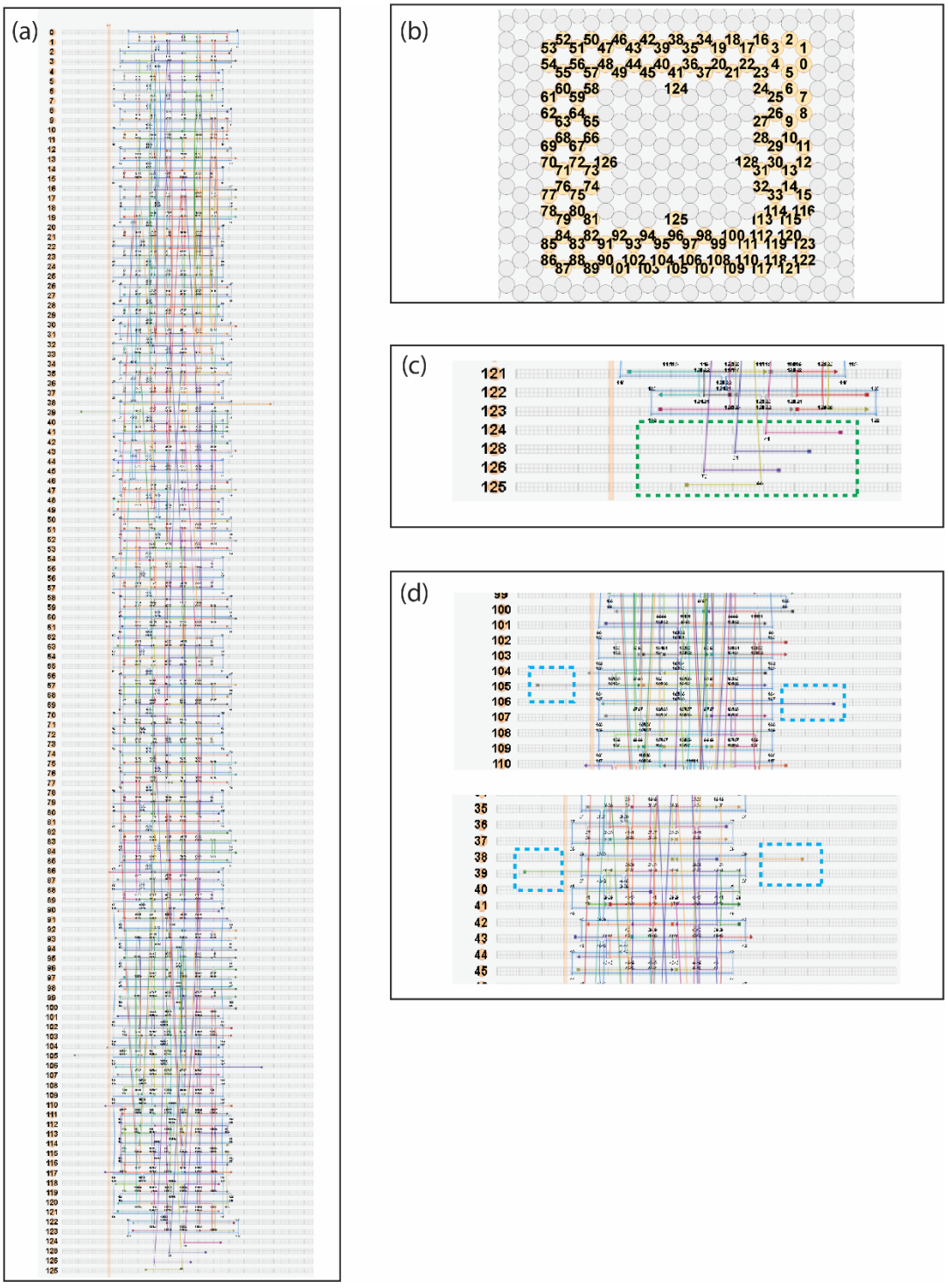

Figure S3. Cadnano design of cage. (a) Map of staple strands (triangle end: 3' end, square end:5' end). (b) Map of honeycomb lattice where helices #123, #124, #125, #128 are added for visualization of inside capture strands located at helices #41, #73, #96, #31 respectively. (c) Inside capture strands (green dashed box). (d) Outside capture strands for 30nm-10nm-30nm and 50nm-10nm-50nm heterotrimers (blue dashed box).

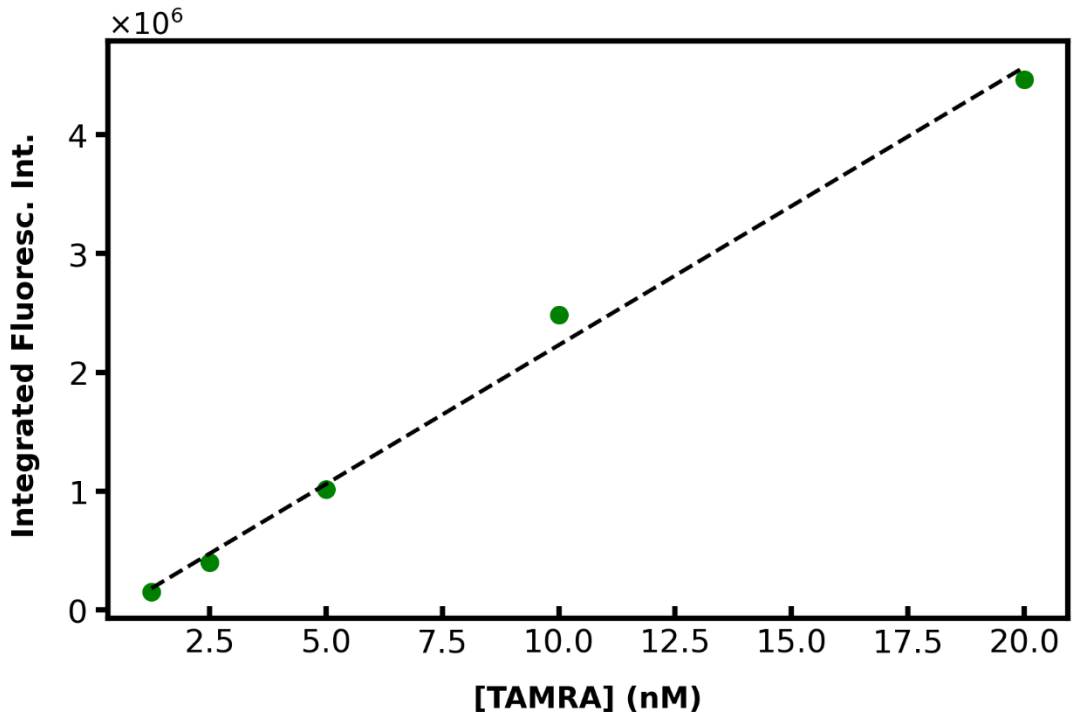

Figure S4. Fluorescence calibration curve of TAMRA.Excitation wavelength = 500 nm. Linear regression equation: y=233945x+239544 and R^2 = 0.9935.

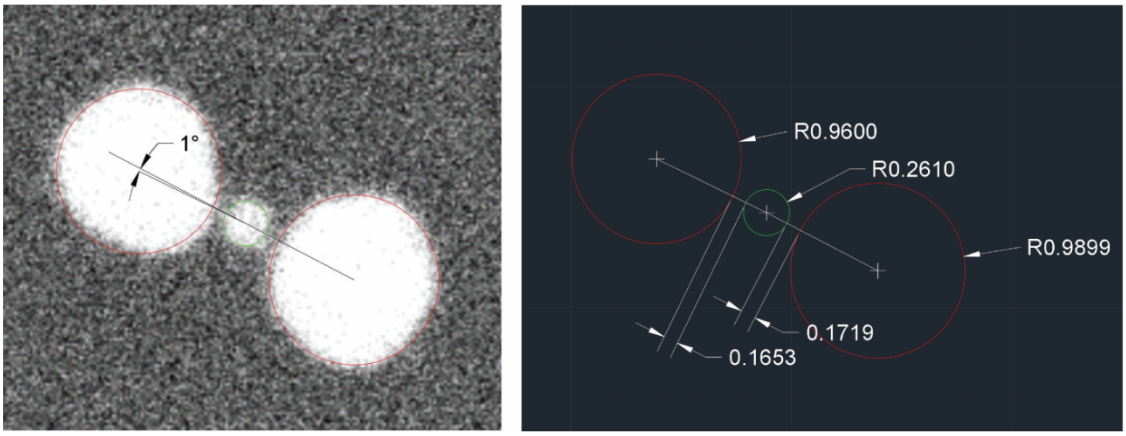

Figure S5. Bending angle and gap distance analysis. Masks were placed on SEM image (shown as green and red circles on the left) using AutoCAD 2019. The bending angle was measured using the measuring tool in AutoCAD 2019. The size of AuNPs and gap distances were measured in AutoCAD (right) and converted to actual values using SEM scale bar.

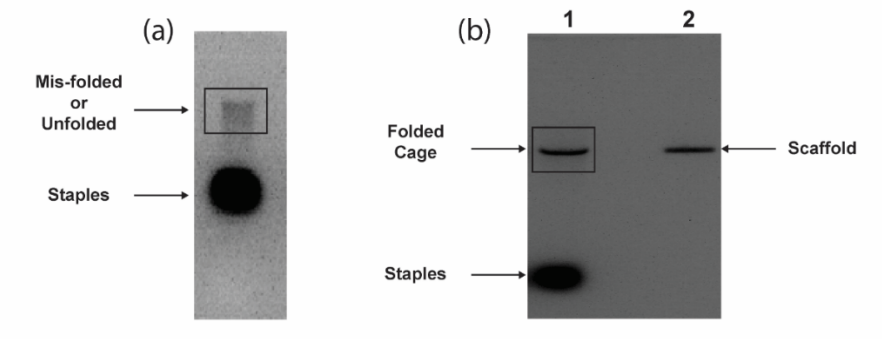

Figure S6. Agarose gel results of cage folding. (a) Ramping rate: −1.5 °C/hr. (b) Ramping rate: –0.2 °C/hr.

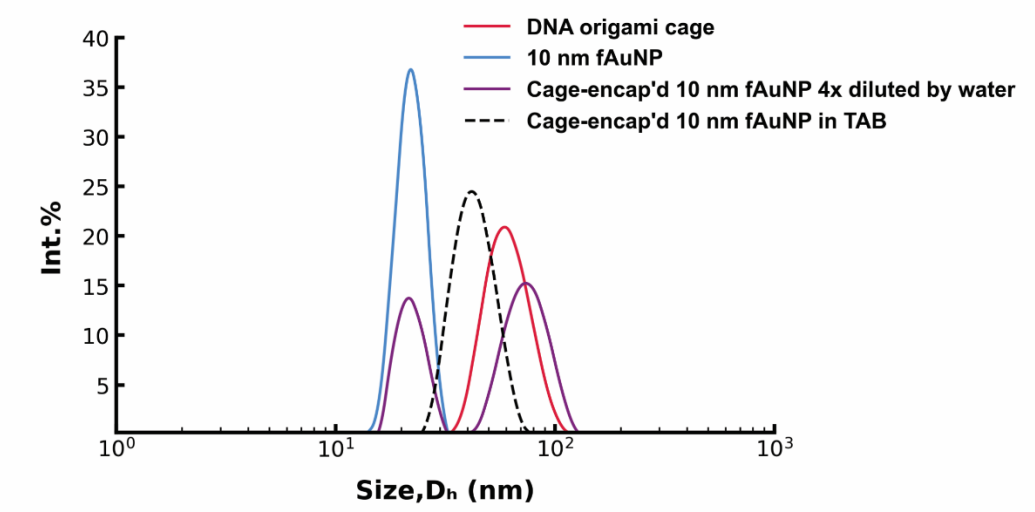

Figure S7. DLS analysis of cage-encapsulated 10 nm fAuNP stability in buffers with different ionic strengths. Neat DNA origami cages and neat 10 nm fAuNPs were also annealed.

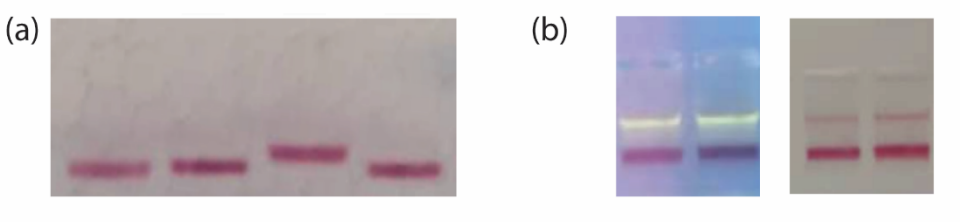

Figure S8. Additional agarose gel results of 30 - 10 - 30 nm heterotrimers.(a) Unstained gel result of 30 nm fAuNP mobilities. From left to right: 30 nm fAuNP in water, 30 nm fAuNP mixed with scaffold DNA in TAB, 30 nm fAuNP mixed with all staples in TAB, 30 nm fAuNP in TAB. The only one that showed slight mobility difference is the 30 nm fAuNP mixed with staples indicating staples might interact with 30 nm fAuNP. (b) Stained gel results 30 -10 -30 nm heterotrimer, the fluorescence signal (yellow-green band) of cage on the left lined up with the slow-moving pink band on the right.

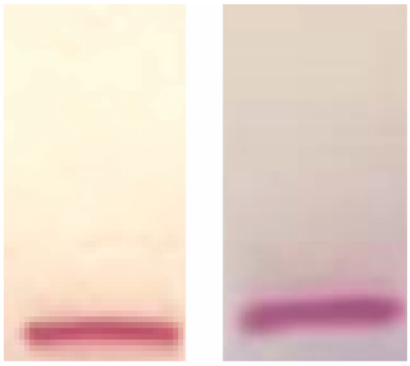

Figure S9. Agarose gel results of control experiments in 30 -10-30 nm heterotrimer assembly. Left: Mixture of 10 nm and 30 nm fAuNPs in TAB at molar ratio of 1:2, only 30 nm fAuNPs were visible. Right: Mixture of 30 nm fAuNPs and an origami cage with noncomplementary outside capture strands, only one unreacted 30 nm fAuNP band was visible.

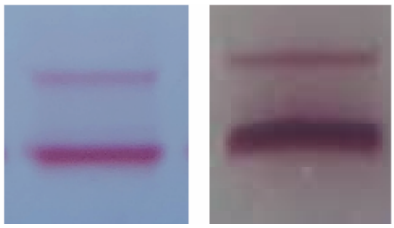

Figure S10. Effectiveness of thermal annealing in 30 nm fAuNP binding. Left: not thermal annealed. Right: thermal annealed. Both are characterized by agarose gel.

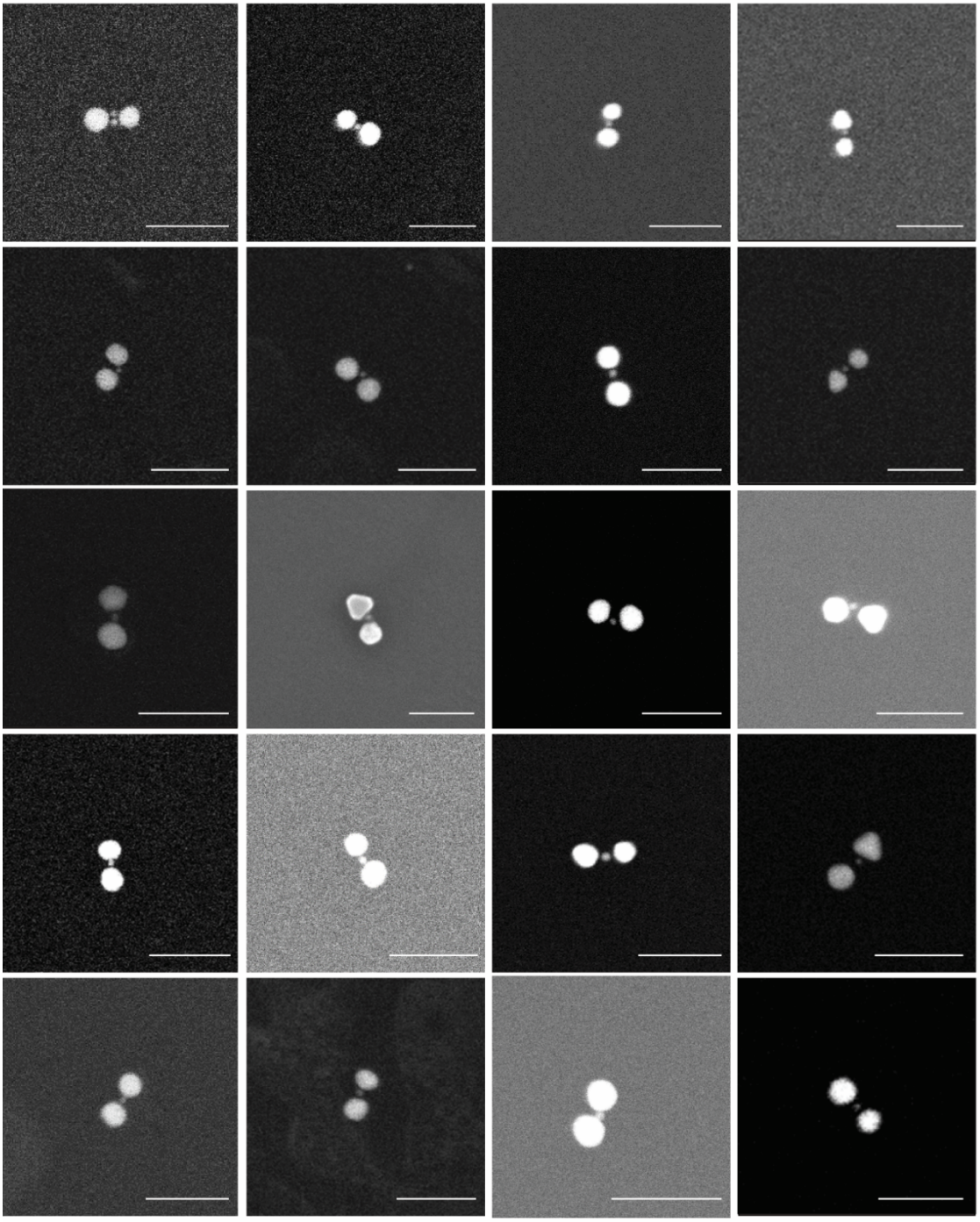

Figure S11. Additional SEM images of 30 -10 - 30 nm trimers. The leftmost one in the first row showed two 10 nm fAuNP flanked by two 30 nm fAuNPs. Scale bar: 100 nm.

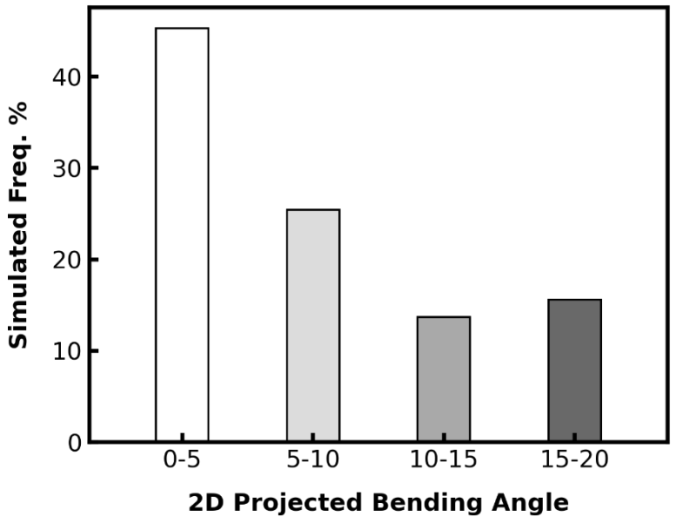

Figure S12. Simulated histogram of 2D projected bending angle of 30 -10 – 30 nm heterotrimers. Heterotrimers with 3D bending angles that have two populations with normal distribution: 7.0°±0.9° and 18°±0.5° could reproduce the histogram in Figure 4(c).

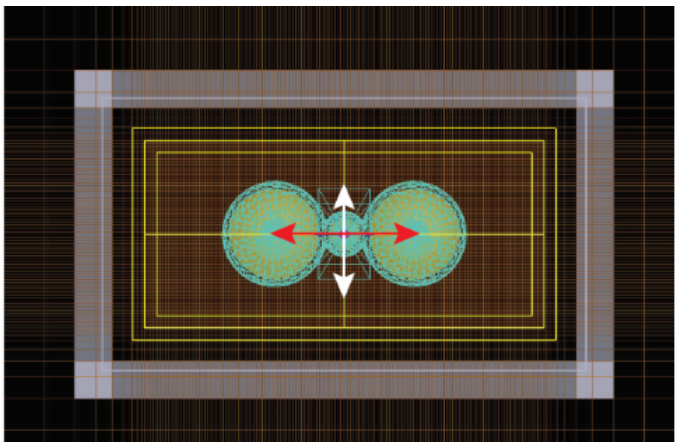

Figure S13. Set-up of FDTD simulation. Red and white double arrows indicated the longitudinal and transverse light polarizations used for simulations.

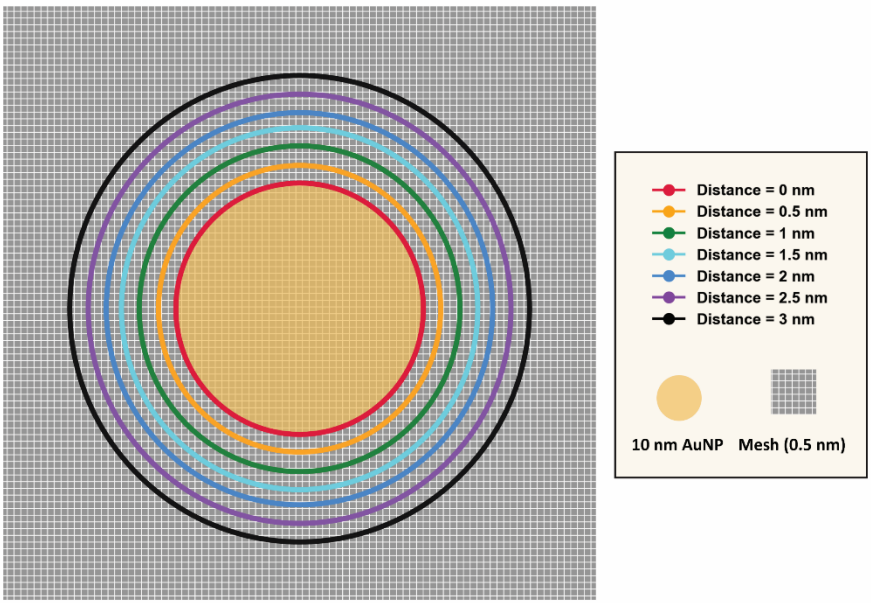

Figure S14. Illustration of FDTD electric field data extraction.

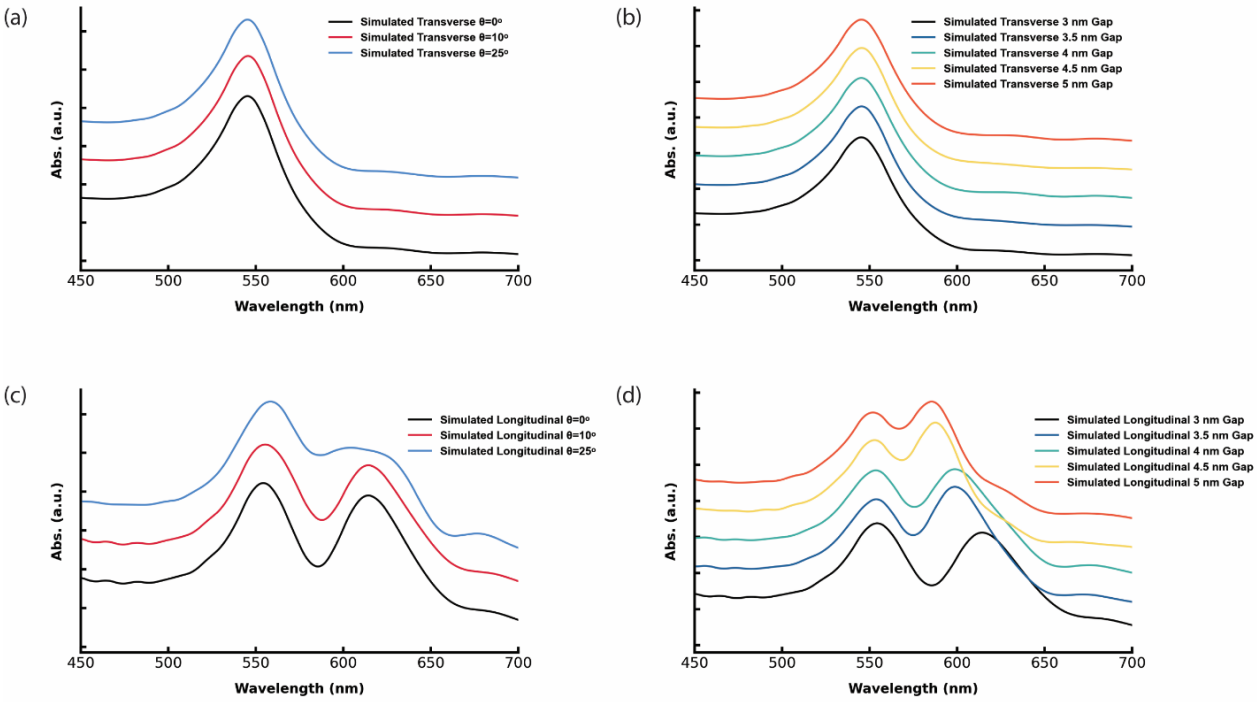

Figure S15. Simulated 30 - 10 – 30 nm heterotrimer absorption spectra. (a) Simulated transverse mode of heterotrimers (3 nm gap) with different bending angles. (b) Simulated transverse mode of heterotrimers ($\theta=0^{o}$) with different gaps. (c) Simulated longitudinal mode of heterotrimers (3 nm gap) with different bending angles. (b) Simulated longitudinal mode of heterotrimers ($\theta=0^{o}$) with different gaps.

The simulated transverse absorption spectra were independent of bending angles and gap distances (Figure S16a-b). The heterotrimer with a 10° bending angle only slightly deviated from perfectly aligned heterotrimer in simulated longitudinal absorption, while greater deviation and blue shift occurred to the heterotrimer with a 25° bending angle (Figure S13c). The longitudinal peak blue-shifted up to 10 nm as gap distances increased from 3 nm to 5 nm (Figure S13d). Besides various polarization angles in experimental measurements, minor gap and bending angle variations in heterotrimer could also produce an absorption spectrum as shown in Figure 6a.

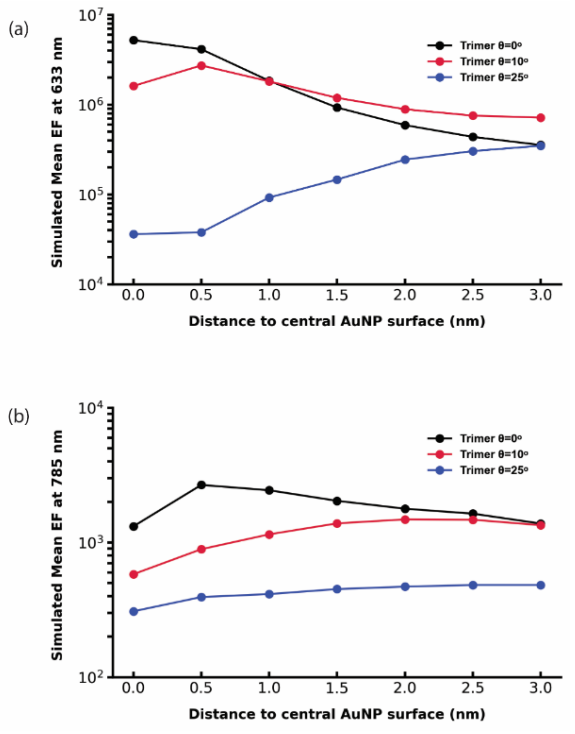

Figure S16. Bending angle dependence of simulated mean EF values of heterotrimer (3 nm gap) with longitudinal excitation at 633 nm and 785 nm.

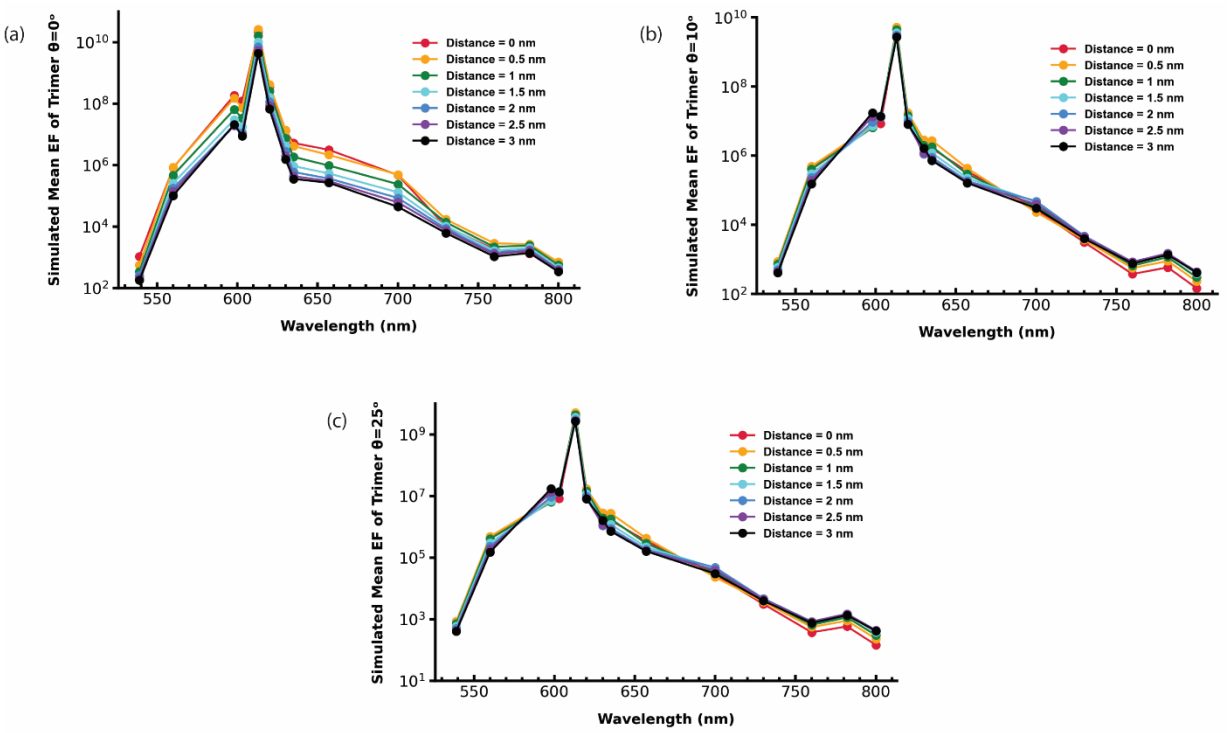

Figure S17. Simulated mean wavelength-dependent EF of trimers (3 nm gap) with different bending angles (a), $\theta = 0^{O}$, (b) $\theta=10^{O}$, c) $\theta=25^{O}$ and at different distances from surface of 10 nm AuNP. Laser polarization is parallel to trimer long axis.

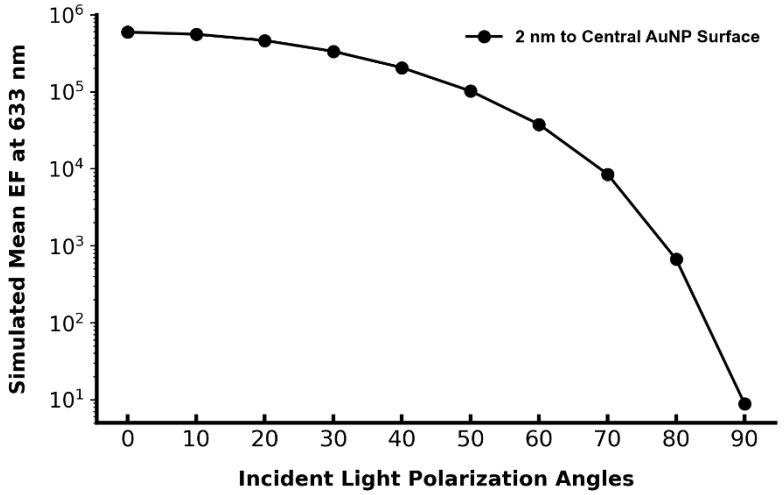

Figure S18. Simulated mean EF of heterotrimer (3 nm gap) as a function of incident light polarization angles.

Custom MATLAB code was employed to analyze electric field values exported from FDTD simulations of the heterotrimers, facilitating the calculation of mean enhancement factor (EF) values, which were subsequently illustrated in Figures S15-17. According to the data presented in Figure S16a, heterotrimers at bending angles (θ) of 0° and 10° exhibited the same trend: the mean EF decreased as the distance from the central AuNP surface increased. Conversely, the heterotrimer with a bending angle of 25° displayed a divergent trend, suggesting that a larger deviation from collinearity significantly impacts the plasmonic properties of the heterotrimer. Interestingly, Figure S16b shows that the three trimers followed similar patterns in their response to varying conditions. The experimentally observed average EF at 785 nm was 1.12×10^3, closely aligning with the mean simulated EF depicted in Figure S16b. Further analysis revealed in Figure S17 indicates that the incident wavelengths have a pronounced effect on the simulated EF values for the trimers: the mean EF peaked at the longitudinal LSPR wavelength (613 nm for $\theta = 0°$ and 10°, 604 nm for $\theta = 25°$) and decreased sharply as the incident wavelength deviated from the LSPR peak. Additionally, Figure S18 demonstrates the significant influence of the polarization angle of incident light on the simulated mean EF values.

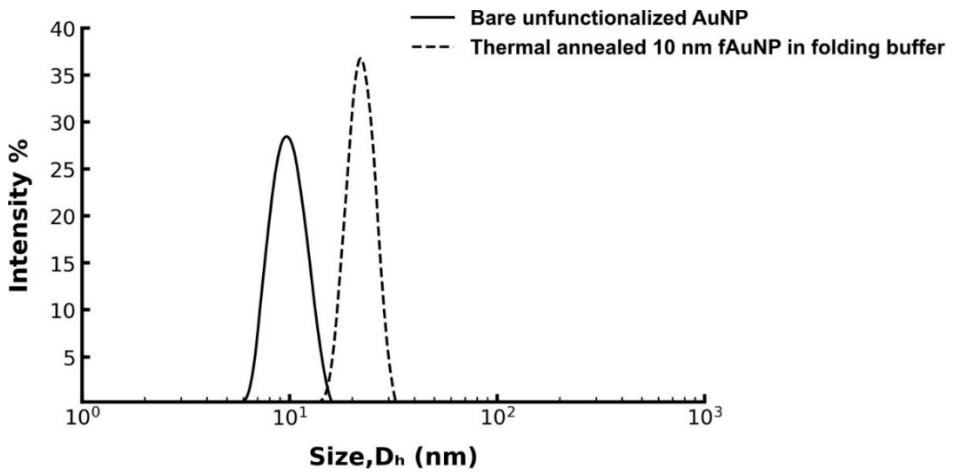

Figure S19. Additional DLS results. As received, unfunctionalized AuNPs have D_h peak at 10 nm. 10 nm fAuNPs remained intact after thermal annealing in the folding buffer as shown by single peak at 22 nm.

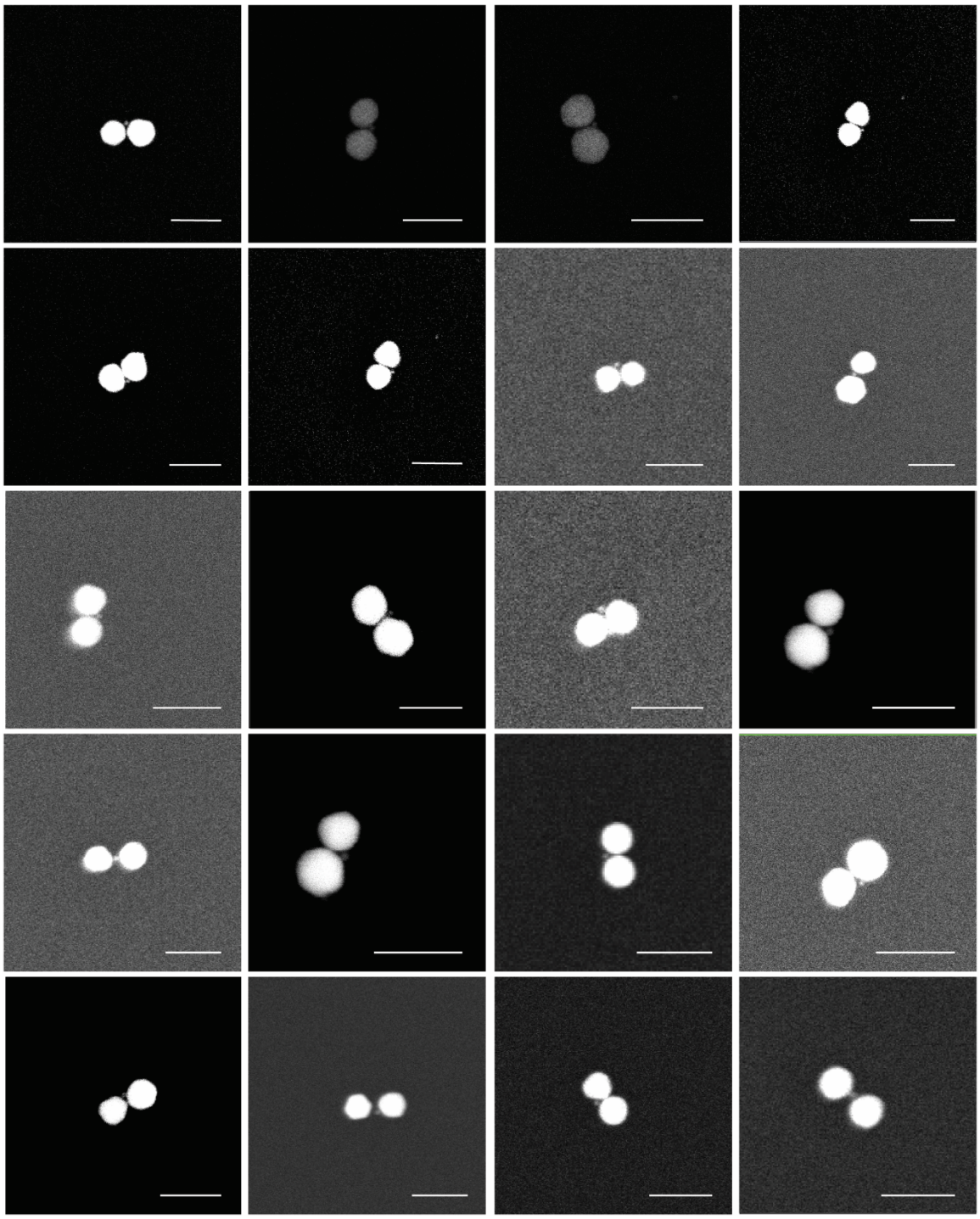

Figure S20. SEM images of 50 - 10 - 50 nm trimers. A backscattering detector was used. Scale bar: 100 nm.

Figure S21. Agarose gel result of mixture of 30 nm, 50 nm fAuNPs and the cage-encapsulated 10 nm fAuNPs.

Figure S22. Agarose gel result of 30 - 10 - 30 nm heterotrimer assembly without NaCl and SDS adjustment.

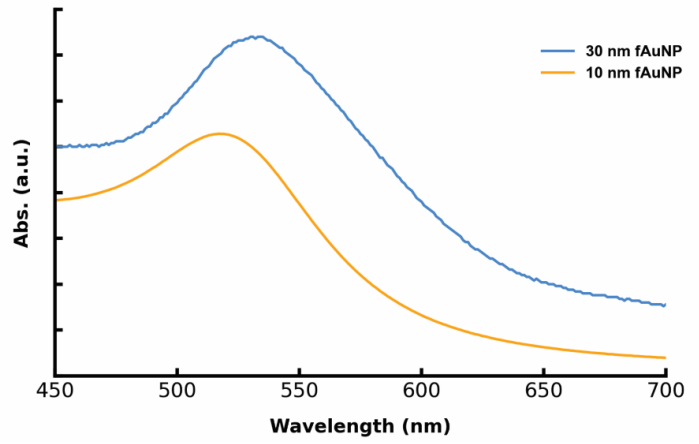

Figure S23. Experimental UV-vis spectra of 30 nm fAuNP (absorption peak at 532 nm) and 10 nm fAuNP (absorption peak at 523 nm).

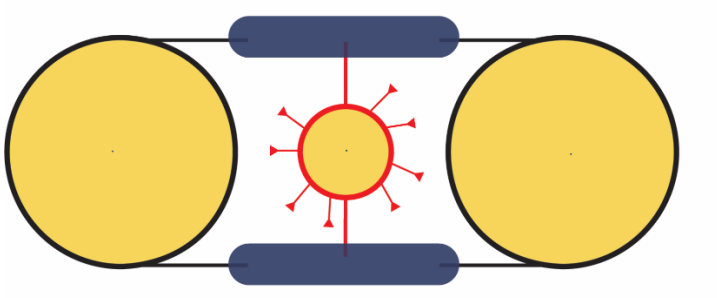

Figure S24. Schematic of heterotrimer contains TAMRA-tagged central nanoparticle. Black line: Outside capture strands; Blue round corner square: Origami cage; Red lines with triangle-end: TAMRA-tagged thiolated DNA ligands; Red lines without triangle end: inside capture strands, only two are shown for simplicity.

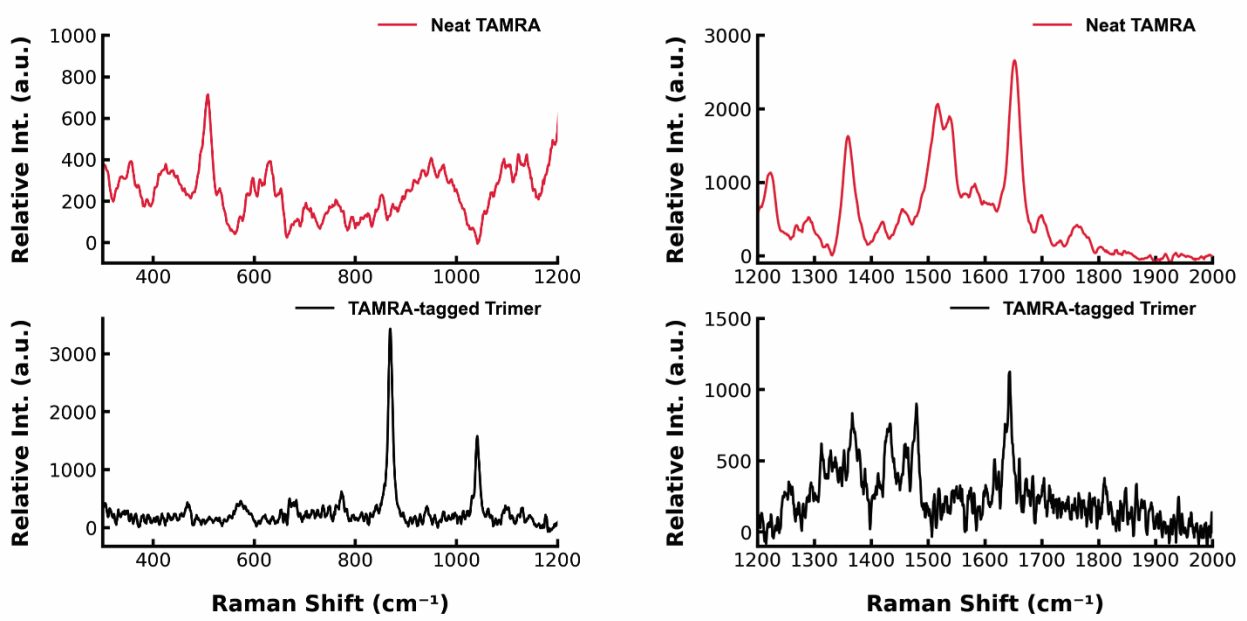

Figure S25. Full SERS spectra of heterotrimer that has TAMRA tagged in the central particle and Raman spectra of neat TAMRA at 633 nm laser excitation. The lower range from 300 to 1200 cm^{-1} on the left and upper range from 1200 to 2000cm^{-1} on the right are shown separately for better peak resolution.

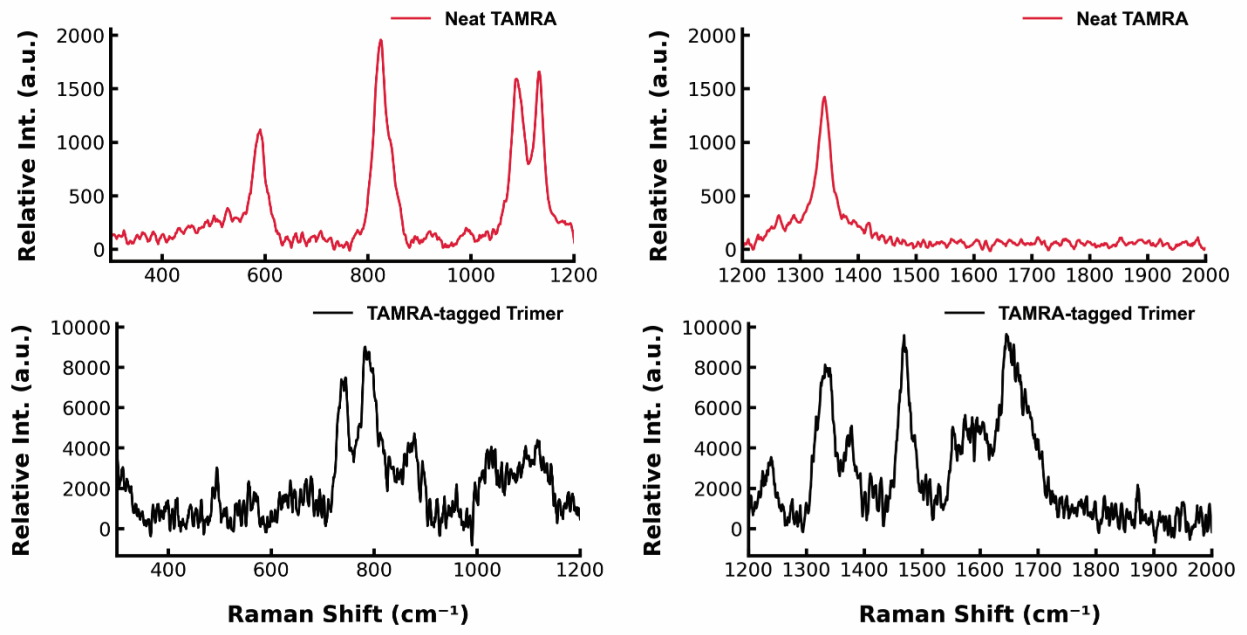

Figure S26. Full SERS spectra of heterotrimer that has TAMRA tagged in the central particle and Raman spectra of neat TAMRA at 785 nm laser excitation. The lower range from 300 to 1200 cm^{-1} on the left and upper range from 1200 to 2000 cm^{-1} on the right are shown separately for better peak resolution.

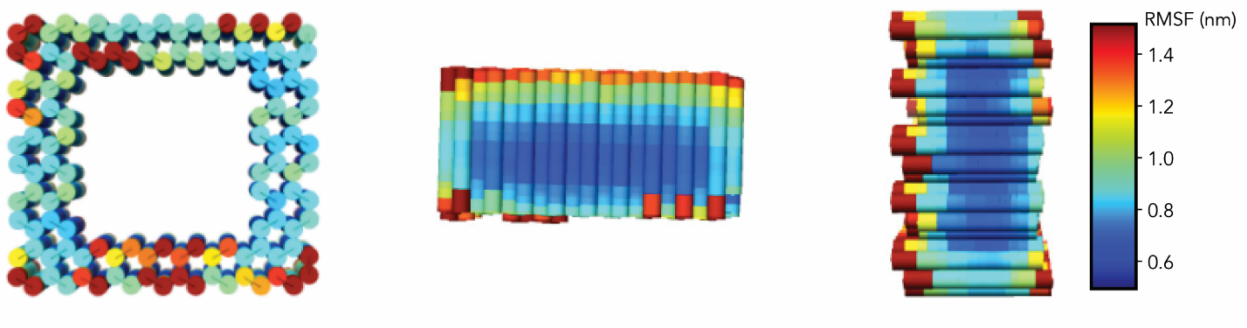

Figure S27. CanDo (https://cando-dna-origami.org) structure and local flexibility predictions of 3D hollow origami cage shown as a heatmap that indicates local root-mean-square fluctuations (RMSFs). Our cage displays good stability with maximum RMSFs value of 1.51 nm, and 95% red region (most flexible) RMSFs below 1.05 nm.

Helix	Sequence (5' to 3')
#39	**gtaaattgcggaat**TTTTCAGGTCATTCGCAAACCTGTT
#105	TGAAAGTAAGAACGGGTATT**gatgtgcctcactacg**
#38	TGAAAGTAAGAACGGGTATT**gatgtgcctcactacg**
#106	**gtaaattgcggaat**TTATCACCAGTAGCCAATGAAACC
#38	TTGCTCCTTTTGATAAGCATACATTTAGAATACCAAAAACGTAGATT **gatgtgcctcactacg**
#106	TGAAAGTAAGAACGGGTATT**gatgtgcctcactacg**

Table S1. DNA sequences of outside capture strands.Extensions are in bold lowercase. The two strands having 3' end extensions are for 30 -10 -50 nm trimers only. 50 nm IPT has no outside capture strands.

Helix	Sequence (5' to 3')
#73	**taatcagcgtttcc**TTTTAAGGCACCCCAGCGGCGCGAAGCGACCT
#41	**taatcagcgtttcc**TTTTCGCGAGCATGCCTGGAAAGGCTCAACCG
#96	**taatcagcgtttcc**TTTTTAAATGTTCCTGTATTTTAACAGCCGAA
#31	**taatcagcgtttcc**TTTTATTCAAGACTCCCCCCATTAGGCCATTT

Table S2. DNA sequences of inside capture strands.Extensions are in bold lowercase.

AuNP Size	Sequence	Notes
10 nm	GGAAACGCTGATTA*TTTT* 3'-SH	-

10 nm	GGAAACGCTGA***T(TAMRA)***TA*TTTT* 3'-SH	**TAMRA** attached to a T
30 nm/ 50 nm	5' ATTCCGCAATTTAC*TTTT* 3'-SH	-
30 nm/50 nm	SH-5'*TTTT*CGTAGTGAGGCACATC	For 30nm-10nm-50nm Heterotrimers
30 nm	5' TAATCAGCGTTTCC*TTTT* 3'-SH	For Figure S4b

Table S3. DNA sequences of thiolated DNAs. 4 italic Ts are spacers, not used for hybridizations.

#	Sequence (5' to 3')
1	TTACAAAGCTGTAGGGTGTCTAATTCTG
2	ACAGGAACGGAATTTTGTTTGGGGATGTGTAAAACGCCAAGC
3	AGGCCTACCCCTTATAAAGGTAACCGAT
4	AATAATAATTTACTACCAGGTTAGGATTAGCGGG
5	ATTACTAGTTTAGTATATACAAGTAATTTTCGCCATAAAGGTAGTCCAGA
6	CGAACGAACAGGCAGTAGCATTTTGGGG
7	ACCGAAGCCCAATAATTATTT
8	ACAACATAATTGTTATGATATCGGAGAC
9	ACTCCTTCATTACCCAAAGTAAGACACC
10	TCAGATATAGAAGGCTTCTAAGAACGC
11	GCCCTAATTAAAAAACCACCAAGTATGT
12	ATAAAGTACCGACAGTAGTCACCAATTTAACCTAGGGCACAGTCC
13	TAGTATTATCCGTCCAGGGAACGGGAGAGCCAAAG
14	TGTTCAGCTAATGCAGATTATCAAGTATCACGATATAAGTATAGC
15	TGTAGCATGTACCGGAACAACTGAAAATATTGTATCGGTTTATCA
16	TTTTAACAAGAGAATATCGCATTAACT
17	ACAAAGCGTGAATAGGTTTAAAATCATT
18	AAAAATGGAAAATAATTACGCGCAGAAG
19	GTGCCCGTACTCATCGAGCCGTTT
20	CGAACGTACCAGAATCAGGCTCTGGCGA
21	AAGGAATATAAAAAGAGAGGCATAGCGTC
22	CTGAGAGAGAGGTGGATTAAG
23	TTTTGAAAATAAGACAGCCATATAAGAGCACAAGATGTACTGTACATGG
24	TTTAAATGCATGAAAAGTTCTACTTAGAGCTATATAATATCGCGCAGA
25	AGAAGGATTTTGTTCGACTTGACAATTT
26	CGGCTGTCATTCCATTAAGAACCTATTATTCTGA
27	ACGGATTCGCCTGATTGAAGATTAGTCAGTATAGTTTGACTTAAC
28	GCCTGATAAATTGTGTCGGAACGATGACCAATTGAGAT
29	ATAGAAAATTTTCATATTACCGCGTTAGAGCGCACCGAGAGAA
30	CGCCAGCCCACCAGCCACCCTACCGGAACCGCCTC
31	TGCCCGCGGAAACCATCCTGAATCATCAAGAAACCTATTAATCGTATTA

32	TGCAACTGGAAGCAGATTAAGAAAGATG
33	GCTTTCGAGGCATCGCCCGATATATTCGGTCTGCGGGAAACGAGG
34	GTTATCTTAGGAGCGCATCGTAAC
35	AAAAGGAAGCTTGATGCGCCGCTTGCAG
36	ATTCAAACGGTTGTAAATCATGTAGATT
37	TTTCCAGAGCCTGAACAGTAATTGGGGAAGGCGGAAATAGAGCCAGCA
38	TAGCAATGGAAAGGTAATAAGAAACGCTCCTACAT
39	GGGCCTGAAAAAAGTAAACACCAACCAA
40	ATTGCATTAATACTAAGCCTT
41	TAAGAATAACAATATCTATTAGGCGAACT
42	ATGCCACAGACAGACGGCTAATTAAAGGC
43	TTTACAAACAATTCGATTTAGTGCCGGAGCCAGCTTTCCGGC
44	ACGTCACACCATTATCATTAACCGTTCC
45	TAAGGCGTTACCAGACGCTCATTAATTGGCCACCCGACAATAAAC
46	CAGTATTGCAACAGAACGCCATTCGCGTCTGGCCTGAGCGAGCGGCGGA
47	AGTTGAAGATTAGAGTCACGTGACAGTA
48	AACGCAACATAAAGTAAATCACACGCCAAACATAACAAATGCTCTTTAC
49	GCAACTTGAGAATCAATCCAACTAACGA
50	TGAATTTAGGACTAGGGTAAAAAACGAA
51	CCAGACCAAAGTACCTCAACATTTTGCG
52	CTTAGCCGAAATCCACAAAGTGTAGCAA
53	ATGGATTACAGATTCCGACCAGGACATTCAGATAGACCTGAAA
54	TTTTAAGAATAATACAATCCAGCCTTAAATC
55	GGAATACCACATTCTTCATCATTAATAAAGGACGTTGGGAAG
56	AAACGAGAATCAAAGACGACGTACGAGGGCAGATA
57	GAACACCCTAATTTAAATAAAAACGATTAACCGAGCTGGCATAGGCGGT
58	GGTTTACCGGGGTCTTAATGCTTTCGGAGGCTGAG
59	TTCATTAGAGAAACGTAGTAAGCGATTT
60	TGAAAGTAAGAACGGGTA
61	GGGTCGAGTGCCAGAGTAGCGGCCGGAA
62	AGGCTTGAGAAAGAAACTAATCATAGTA
63	AGAACGCTTTCAAATTAATTTCGGAATC
64	CCTCAGAGAATTAGGATTCCCGGAAGTTAGCTTCA
65	TTTTTGTAATACAATGCAAATATAAAGGCCACAG
66	AGAGGCACTAAAACAGATTTGTAT
67	GGCAAATTGAAAAATAATGGGTCAACAT
68	GCTAAATAGGGTGAAGTAATGGATAAAA
69	GCTGCAAACGCCAGGCGCAACCAAAGCGATAATAC
70	CGTAATCACGCAAGTGTAGGTATTTTCA
71	AGTACATCCTTTATAACTCCAACATATA
72	TCTTTTCCGCGCGGCCAGCTGTGCGTTGAATGAGT
73	TACCAACCCAGCTCGGGAGG

74	AGAGCAAACCCTCGTTTTGCCATAGTAAAATGTTTCATAAATGTTCAGA
75	CCTTATTTCATCGGAGAGCCGATTGACA
76	TGAGGGAAGCGCTAGATAACCCAAGAAA
77	GCCACCCCACCCTCCATTTTCAATCAAG
78	AATCATAGGTTCGCAAGTATGTAATTCTGACTGGTTTGCGTGTGAT
79	TGCTCAGGAGCATGTCAATAAT
80	GACATTCGAATTATGACTTGACACCTTATCTTTAGACATCCT
81	CCTTTTTAGTACATAAAT
82	TAATTTTTTCACGTTAAAGGAACAACTTAATTTTCTGTATGG
83	TAGCTATAACCCTGTATGAAGTTAATGCCGAATAA
84	GTTTGAGATTTTGCAAGGGCGGCCTCTT
85	AATACCCAAAAGAAGAAACGCAAAAGTACTATCTT
86	AATTATTCATTTCAATTCCGAAAGAAGCGAA
87	CCAAAAAAATTACAAAACAAACATCAAGAACAGTACGGGAGAAAC
88	ATAAAAGAGTCACAACTTTACACAATAGCAAGC
89	CCCTGACCCCAAATCTTGACA
90	ATAAAACCCAGCAGGCTCATTGCCAGCTT
91	AACCAAGTACCGTCACCCACCGCATAAACAGAGTGCCTTGAGTAA
92	GATGGGCACTAACAATTTGAGGACAACTTTTAAAA
93	AGAAGGACGGATAAGAGGGTTCGGCCAC
94	GAATCGTAGACTGGTTTTGCATAACGGATACAGGT
95	AGAACCGTGACAGAAGAGGCACATGTTA
96	TATTTCAATTAGCTGAGGGGGAAATTATTTGCACG
97	TAGGGCACAAATATTCATATTTATTTT
98	GCCACCAGAGTTTCCAAACTAAGTTTTG
99	CAAACCCTCAATCATTGCTGAGAACAAATAACAACCCGTCGG
100	TACCGTCTTAAATATACCGACAAATACG
101	TAACATCAGGTCATTGTTTTACTTTGAACAAAAGA
102	ATTATTCATGCTGAGATTGGGTTAGGTA
103	ATAGCAGCACTTAGCGTCGCGTTTAGCGTTTGCC
104	TAGAAAGTAACACTCCCTCAT
105	GGAAGCAAGCCTGGCGACGTT
106	TATTCCTTCACCGCTGGTTTT
107	TTAGAACGGTCATTCTGGAGCATCGATGGTAAAACATCATAT
108	CCCGGTTAAAGCCCAAGATTGTATTTAA
109	TTTGGGCCGTATTGATAGTCGTTTCCAC
110	TCATTATACCTTATATTGGGCCTTTGAA
111	GCATCAAAGGAAGCACCTGAGTACCAAG
112	GGCAATTCATAAGTTGGGGTTTTCGTCGACTCTA
113	GACGTTAGATCTAACAACGCC
114	GGCTTTGCTTAAACGCCTTTACTCCAAACTACCAGCCGGACAATAGCCC
115	CATCTGCCAGTTTGAGGCACTCCAAACCAGGTGTTGGGGGAACAA

116	GGGAATTTATTCATAGCGTCAGTAATAAG
117	CGTCAGACACCCACTCAGAACCTCAGGAGGTTTAG
118	TTCCATAAATGATATACTGCG
119	ATCCAGTGACGGCACTACCATTTCTGAATAATGGA
120	TTGCTCCTTTTGATAAGCATACATTTAGAATACCAAAAACGTAGA
121	TCGGCCAAACCAGTGCAGCTGATTGCCCTGATTATCAGA
122	ATCCCCGGGTGAACCCTCAT
123	TTTCAGGAAAATCAAGCCACCCAGAACC
124	CTCATAGTTAGCGTAACGTAAATGTCAACAGCAACAAC
125	TCGAGCCTTTTCGTCCAACATATATAGT
126	ACTAATAAGGAATTGTCAGTT
127	ACTTCAAAAGCAAATCTTTACTTAAACAATTCATTGAATCCC
128	ATTGTAATAAAGCATCATAGCTGATAAA
129	AGTTTCCATTAAACAAGACTTGCATCGGTCGTCACCCTCAGC
130	CGGTTTGGCCAGGGCATTGCA
131	TGAACGGTTTGACCCAACCTAATACGTA
132	TATCAATAAGAGAGCGATAGCTGATAGC
133	GCAATAGAGCAGATCAATAGGTGCCACGCATCACCATATCTGGAGGAAG
134	TCAGATACGCCACCAAAAAGGAAGAGAA
135	ATATATGTGAGTTAGATT
136	CAAAATTTAACCTTATCGTCGATTTTCC
137	AATCCTTTCAATAGCCATTCGCCTCAGG
138	ACAACGGACTCATCTGTACAGGAGTAATCAACGTA
139	GATGGCTAATAGTAAGGCAAAGCATAAA
140	GAATTTAAGCCAGATCACAAACAGGTCA
141	CGCTTTGCTGAGGACAATGATTTCAGCGGAGTCGCTTTCCA
142	ATTTTTAACCGAGCTGTGTGAACGAGCC
143	TTCTAGCTGTTTCCTCGAATTTTGCATG
144	TTAGTTGCTATTTTGCACGCTAACGAG
145	CCTGCAGCCAGTCAGGTGCCTCGCTCAC
146	ACAGAGAATTTTTGAAAGGCT
147	TTTCATAATCGATAGCAGAACCCATTCCACAGAC
148	CGTGGCGTGTCTGAACCCTCC
149	CGAAACTAATGAAACAATTTCATTTGA
150	ACCAGGATGAAAACCCAATTACTATTAA
151	ACGCTGAGAGTGAATTTA
152	ATCCCAGGGCCTGTACGCGTCGAACCGC
153	ACAAATACAATGGGAATTACAGCCAGAACTGAATCT
154	TTTGCCTCGTAATCGTTGAGGCAAATAA
155	GTGAATTACCAGTCAACGAACAAAGAAGTTTACCAAATCAGGGCGGATT
156	AAAGAGAAAACAGGGAATTGGTTTACTTACGCTCAATCGTCT
157	CATAACGATATTATACAACAGAACTGGC

158	AAGATCGGGACGACTGGTGTATTGACCGTCTAAAG
159	CTGACCTTCATCAAACCAGGCACCGAACGGCGCAGACGGTCA
160	GAATCCTGAGACTACTCCGGCTTATATA
161	CGCTATTGGCGATTCAATATATGTCGTGGGAGAGG
162	TCTCAGAGATAAGGCCTGTCA
163	CGTTTTAGCGAACCTCCTAACGTCTAACATAAATAAGT
164	TAGTCAGATATCGCGTTT
165	CACATTAATCATTAATGATT
166	TTCAGAGCCGCGACGATTGGTT
167	TAATTCGTCATTCCATTT
168	CTTCTGGAAGTATTTTATCTTAAAATTT
169	TTTTTGTAGCAGACTTTT
170	AACAGTTCAAAATTTTATCAAGTGGCTT
171	TTAAATCTACGGTTGAGA
172	TTCAGATGAAGGAGAGTACCT
173	CATCAATATCCGCTCATT
174	TTGCAGTCTCTCTTTTGATGTT
175	TTTTGAATCCGTAGTTTT
176	TTGGAATAGGTCAATAGAACAAGAAA
177	TTTCTCCGTGGACCTCAAATTT
178	TTTGTAAACGTTTAAAATTTTTTGTGTGGCAAAAACGTAAAAATAGCATT
179	TTATACAGGAGATTGAGT
180	TTCCTTGATATATGGAAAGCTT
181	TAAGGGAGCATAGGCTTT
182	TTCGAAAGACATTTCATGAGTT
183	TTTCAGAGCCGAACCACCACTT
184	TTTTAGAGGAAGTCTTTT
185	TTTTTTGCTAAATTGCGAATTT
186	TTCAATTCCACGAGCTAACTTT
187	AGAGGCAAGTAATAAGAGATT
188	TTTCAAATGCTCCTGACT

Table S4. DNA sequences of unmodified staples.

Neat TAMRA 785 nm	**Neat TAMRA 633 nm**	**Trimers 785 nm**	**Trimers 633 nm**	**Origin**	**Assignment** [1-5]
649 cm^{-1}	1652 cm^{-1}	1647 cm^{-1}	1642 cm^{-1}	TAMRA	C-C stretch xanthene ring
-	1582 cm^{-1}	1586 cm^{-1}	-	TAMRA	C=C ring stretch
1567 cm^{-1}	1562 cm^{-1}	1554 cm^{-1}	-	TAMRA	N-H bend
1534 cm^{-1}	1537 cm^{-1}	1529 cm^{-1}	-	TAMRA	amide II
1515 cm^{-1}	1517 cm^{-1}	-	-	TAMRA	C-N stretch, C-H bend, N-H bend
1509 cm^{-1}	-	-	-	TAMRA	ring vibration, C=C in plane vibration
1498 cm^{-1}	-	-	-	-	-
1455 cm^{-1}	1455 cm^{-1}	1469 cm^{-1}	1477 cm^{-1}	TAMRA	ring vibration
1414 cm^{-1}	1417 cm^{-1}	1415 cm^{-1}	1433 cm^{-1}	-	N-C stretch
1356 cm^{-1}	1360 cm^{-1}	1376 cm^{-1}	1366 cm^{-1}	TAMRA	C=C stretch xanthene ring
1287 cm^{-1}	1289 cm^{-1}	1333 cm^{-1}	-	TAMRA	N-H bend, CH_2 wag
1266 cm^{-1}	1267 cm^{-1}	-	1253 cm^{-1}	TAMRA	C-O-C stretch
1219 cm^{-1}	1223 cm^{-1}	1235 cm^{-1}	-	TAMRA	-
1189 cm^{-1}	1190 cm^{-1}	-	-	TAMRA	-
-	1123 cm^{-1}	1118 cm^{-1}	1129 cm^{-1}	TAMRA	C-H in plane bending
962 cm^{-1}	-	962 cm^{-1}	-	-	-
-	-	866 cm^{-1}	869 cm^{-1}	DNA	P-O5 + ribose ring breathing
842 cm^{-1}	852 cm^{-1}	-	842 cm^{-1}	TAMRA	-
-	-	782 cm^{-1}	785 cm^{-1}	DNA	Poly(dG-dC)
757 cm^{-1}	762 cm^{-1}	-	772 cm^{-1}	TAMRA	C-H bend out of plane
739 cm^{-1}	742 cm^{-1}	739/745 cm^{-1}	736 cm^{-1}	TAMRA	-
698 cm^{-1}	702 cm^{-1}			TAMRA	-
677 cm^{-1}	674 cm^{-1}	677 cm^{-1}	670/677 cm^{-1}	DNA	Thymine
-	652 cm^{-1}	656 cm^{-1}	653 cm^{-1}	TAMRA	C-H out of plane bending
642 cm^{-1}	630 cm^{-1}	637 cm^{-1}	636 cm^{-1}	DNA	C3'endo anti-thymidine
627 cm^{-1}	628 cm^{-1}	625 cm^{-1}	621 cm^{-1}	DNA	Guanine + ribose ring breathing
610 cm^{-1}	610 cm^{-1}	617 cm^{-1}	-	TAMRA	aromatic C-C stretch
570 cm^{-1}	572 cm^{-1}	573 cm^{-1}	572 cm^{-1}	TAMRA	-
555 cm^{-1}	-	557 cm^{-1}	-	-	-
-	532 cm^{-1}	532 cm^{-1}	532 cm^{-1}	-	-
500 cm^{-1}	506 cm^{-1}	493 cm^{-1}	-	TAMRA	-
-	-	486 cm^{-1}	486 cm^{-1}	DNA	-

Table S5. TAMRA peak positions and assignments.633 nm and 785 nm excitation wavelengths.

	Mean Value	**Standard Deviation**
Diameter of Large AuNP in Trimer	29.4 nm	2.8 nm
Diameter of Small AuNP in Trimer	7.9 nm	0.9 nm
Gap Size	3.7 nm	1.5 nm
Bending Angle	9.7^{o}	6.9^{o}

Table S6. Statistical summary of SEM image analysis of 30 -10 – 30 nm trimers.

	Mean Value	Standard Deviation
Diameter of Terminal AuNP	46.3 nm	3.8 nm
Diameter of Central AuNP	7.7 nm	1.4 nm
Gap Size	3.5 nm	1.8 nm

Table S7. Size measurements of 50 -10 - 50 nm heterotrimer.

Supporting References

1. Gong, T.; Kong, K. V.; Goh, D.; Olivo, M.; Yong, K. T. Sensitive surface enhanced Raman scattering multiplexed detection of matrix metalloproteinase 2 and 7 cancer markers. *Biomed Opt Express* **2015**, *6* (6), 2076-2087.
2. Prinz, J.; Heck, C.; Ellerik, L.; Merk, V.; Bald, I. DNA origami based Au-Ag-core-shell nanoparticle dimers with single-molecule SERS sensitivity. *Nanoscale* **2016**, *8* (10), 5612-5620.
3. Prinz, J.; Matković, A.; Pešić, J.; Gajić, R.; Bald, I. Hybrid Structures for Surface-Enhanced Raman Scattering: DNA Origami/Gold Nanoparticle Dimer/Graphene. *Small* **2016**, *12* (39), 5458-5467.
4. Yang, J.; Palla, M.; Bosco, F. G.; Rindzevicius, T.; Alstrøm, T. S.; Schmidt, M. S.; Boisen, A.; Ju, J.; Lin, Q. Surface-Enhanced Raman Spectroscopy Based Quantitative Bioassay on Aptamer-Functionalized Nanopillars Using Large-Area Raman Mapping. *ACS Nano* **2013**, *7* (6), 5350-5359.
5. Clark, R. J. H.; Hester, R. E. *Spectroscopy of Biological Systems*; Wiley, 1986.